



## Function and dynamics of *slam* in furrow formation in early *Drosophila* embryo <sup>☆</sup>



Sremukta Acharya <sup>1</sup>, Philip Laupsien <sup>1</sup>, Christian Wenzl, Shuling Yan, Jörg Großhans <sup>\*</sup>

Institut für Entwicklungsbiochemie, Universitätsmedizin, Universität Göttingen, Justus-von-Liebig Weg 11, 37077 Göttingen, Germany

### ARTICLE INFO

#### Article history:

Received 28 May 2013

Received in revised form

11 December 2013

Accepted 13 December 2013

Available online 22 December 2013

#### Keywords:

*Drosophila*

Blastoderm

Cellularization

Endosome

Centrosome

Cleavage furrow

### ABSTRACT

The *Drosophila* embryo undergoes a developmental transition in the blastoderm stage switching from syncytial to cellular development. The cleavage furrow, which encloses nuclei into cells, is a prominent morphological feature of this transition. It is not clear how the pattern of the furrow array is defined and how zygotic genes trigger the formation and invagination of interphase furrows. A key to these questions is provided by the gene *slam*, which has been previously implicated in controlling furrow invagination. Here we investigate the null phenotype of *slam*, the dynamics of Slam protein, and its control by the recycling endosome. We find that *slam* is essential for furrow invagination during cellularisation and together with *nullo*, for specification of the furrow. During cellularisation, Slam marks first the furrow, which is derived from the metaphase furrow of the previous mitosis. Slightly later, Slam accumulates at new furrows between daughter cells early in interphase. Slam is stably associated with the furrow canal except for the onset of cellularisation as revealed by FRAP experiments. Restriction of Slam to the furrow canal and Slam mobility during cellularisation is controlled by the recycling endosome and centrosomes. We propose a three step model. The retracting metaphase furrow leaves an initial mark. This mark and the border between corresponding daughter nuclei are refined by vesicular transport away from pericentrosomal recycling endosome towards the margins of the somatic buds. Following the onset of zygotic gene expression, Slam and Nullo together stabilise this mark and Slam triggers invagination of the cleavage furrow.

© 2013 The Authors. Published by Elsevier Inc. All rights reserved.

### Introduction

*Drosophila* cellularisation is a specialised form of cytokinesis and transforms the syncytial into a cellular blastoderm. Embryonic development starts with a series of 13 rapid nuclear divisions that take place in a common cytoplasm without cytokinesis (Foe et al., 1993). In interphases of the syncytial divisions 10–13, the nuclei together with their associated centrosomes shape the surface of the overlying embryonic plasma membrane by triggering the formation of actin-rich somatic buds. During mitosis, transient invaginations of the plasma membrane, so-called metaphase furrows, extend towards the interior of the embryo to separate adjacent mitotic spindles. These metaphase furrows retract during telophase. A developmental switch occurs after the last nuclear division at the onset of interphase 14. The plasma membrane

starts to invaginate at the margins of adjacent somatic buds. At the site of prospective invagination, the membrane transforms into a hairpin-like canal, which is called furrow canal. It is unclear whether the interphase furrow forms *de novo* or builds on information derived from the metaphase furrow. Concomitantly to furrow formation, the plasma membrane becomes polarised.

Genetic analysis showed that two processes, organisation of the cytoskeleton and membrane trafficking, largely ensure proper invagination of the plasma membrane during cellularisation. Cytoskeleton organisation is controlled by factors such as Rho1, RhoGEF2, Dia and Abl (Crawford et al., 1998; Afshar et al., 2000; Grevenko et al., 2003; Großhans et al., 2005; Padash-Barmchi et al., 2005). Membrane trafficking includes the polarized insertion of new plasma membrane to permit the enormous increase in membrane surface as well as the regulation of endo- and exocytosis. Not surprisingly, many key regulators of membrane trafficking have an important function during cellularisation. For example, the recycling endosome, which is controlled by *rab11* and *nuf*, is required for cellularisation (Rothwell et al., 1998; Riggs et al., 2003; Pelissier et al., 2003) and accumulation of RhoGEF2 (Cao et al., 2008).

As these components are present throughout early development, they do not trigger furrow invagination in interphase 14. Zygotic

<sup>☆</sup>This is an open-access article distributed under the terms of the Creative Commons Attribution-NonCommercial-No Derivative Works License, which permits non-commercial use, distribution, and reproduction in any medium, provided the original author and source are credited.

<sup>\*</sup> Corresponding author.

E-mail address: [jgrossh@gwdg.de](mailto:jgrossh@gwdg.de) (J. Großhans).

<sup>1</sup> Equally contributing authors.

genes are likely candidates for a trigger. Genes such as *nullo*, *slam*, *bnk* and *sry- $\alpha$*  are candidate genes. Previous studies revealed a role of *slam* in furrow invagination (Lecuit et al., 2002; Stein et al., 2002) and recruitment of Patj and RhoGEF2 (Wenzl et al., 2010). Mutations in *nullo* and *sry- $\alpha$*  are characterised by an incomplete hexagonal membrane array and the presence of multinuclear cells (Schweisguth et al., 1990; Rose and Wieschaus, 1992; Hunter et al., 2000). Furthermore, *nullo* controls the separation of lateral and basal compartments and actin-dependent stabilisation of the basal membrane (Sokac and Wieschaus, 2008a, 2008b).

Whereas the mechanisms underlying the invagination process have been intensively studied over the past few years, the initial events of furrow invagination are still poorly understood. Slam is key to understanding furrow invagination. Slam is an early marker of the furrow and is required for proper furrow invagination. As only an initial analysis of the *slam* function has been previously reported, we defined the null phenotype of *slam* and investigated the dynamics and spatial restriction of Slam protein.

## Results

### *slam* is essential for furrow invagination

*slam* was identified by its role in accelerating furrow invagination during cellularisation (Stein et al., 2002; Lecuit et al., 2002). It has remained unclear whether Slam would control the speed of invagination and also be involved in the definition of the site of invagination. The full function of *slam* has not been revealed, so far. No *slam* mutation deleting both maternal and zygotic contribution has been available. Previously, *slam* mutants were generated by zygotic deficiency, depletion by RNAi or with a hypomorphic point mutation (Stein et al., 2002; Lecuit et al., 2002). To clarify *slam* function, we generated a synthetic deletion of the *slam* locus. A large *slam* deficiency was complemented with transgenes for the distal and proximal regions except *slam* (Fig. 1A). Half of the embryos from germline clones with this deficiency crossed to males heterozygous for a *slam* deficiency are devoid of any maternal and zygotic *slam* contribution. These embryos were recognised by the absence of Slam staining or by the absence of  $\beta$ -galactosidase staining from a reporter on the balancer chromosome in the males. Addition of a transgene with 8 kb of the *slam* locus complemented the lethality and embryonic phenotype of the synthetic *slam* deficiency. Previously, the assigned mutant phenotype of *slam* was slow and delayed furrow invagination. In contrast to this, we found that no furrow invagination was visible in embryos devoid of maternal and zygotic *slam* (Fig. 1B, C). In embryos with only maternal *slam* (zygotic phenotype), an incomplete furrow was formed as previously described (Lecuit et al., 2002; Stein et al., 2002). In embryos with only zygotic *slam*, the furrow extended almost to normal length, and some embryos even completed cellularisation. Invagination speed is not dose dependent, as two copies of the *slam* genomic transgene ( $4 \times$  *slam*) did not accelerate invagination (Fig. 1B, C).

Failure of invagination may be due to defective furrow extension or to impaired furrow specification. To distinguish these two options, we stained fixed embryos for a series of markers for the furrow and directly compared embryos with and without zygotic *slam* rescue (Fig. 2). We found by such stainings that several markers (F-actin, Dia, Nullo, Dlg) were arranged in a pseudo-hexagonal pattern in *slam* deficient embryos comparable to the rescued embryos, at least in a qualitative manner (Fig. 2A–D, F, G). In contrast, MyoII (Fig. 2E) and as previously shown, RhoGEF2 and Patj (Wenzl et al., 2010) depended on *slam*. These stainings demonstrate that the spatial information for the site of invagination

and initial steps in assembly of the furrow are at least partially independent of *slam*.

### *slam* and *nullo* together control the hexagonal array of furrows

As *slam* is not required for specification of furrow, *slam* may not be involved or may redundantly act with additional factors. A candidate for such a redundant factor is the zygotic gene *nullo*. *nullo* acts redundantly to RhoGEF2 (Großhans et al., 2005) and RhoGEF2 localisation at the furrow canal depends on *slam* (Wenzl et al., 2010). Thus, we expected that *slam nullo* double mutants may show a stronger phenotype than the single mutants. We generated embryos that were maternally and zygotically deficient for *slam* and zygotically deficient for *nullo* (Fig. 3A). We stained for the furrow marker Dia, which neither depends on *slam* nor *nullo* (Fig. 3A). In contrast to single mutants, Dia did not mark a hexagonal array in *nullo slam* double mutants (Fig. 3A). Instead, large accumulations of Dia and a severely disrupted furrow array were observed (Fig. 3A). These embryos developed normally through the syncytial blastoderm as observed by time lapse recording with bright field optics (data not shown). This observation is consistent with a function of *slam* and *nullo* mainly in cellularisation.

We cannot exclude the possibility that the large Dia punctae represent a degenerated furrow array. This would indicate that another factor is involved in furrow site specification beside *slam* and *nullo*. However, it is clear that *slam* and *nullo* contribute to specification of the furrow array in a redundant manner. We recorded the dynamics of E-CadherinGFP in embryos depleted for *slam* and *nullo* by dsRNA injection to confirm this finding (Fig. 3B). Consistent with previous reports, *slam* or *nullo* phenotypes could be induced in the majority of embryos injected with dsRNA directed against *nullo* or *slam* (Lecuit et al., 2002; Großhans et al., 2005; Wenzl et al., 2010). Although these embryos are not genetically defined null mutants, their phenotype comes close to the double deficiency phenotype. E-CadherinGFP is quickly organised in a pseudo-hexagonal pattern in embryos that were depleted for either *slam* or *nullo* by RNAi. In contrast, this organisation is completely lost in embryos that were depleted for *slam* and *nullo* (Fig. 3B). Similar to the genetically defined double mutant embryos, the embryos injected with RNAi developed normally until cellularisation (data not shown).

### GFPslam distinguishes "old" and "new" furrows

Next we analysed the dynamics of Slam protein. Slam is prominently enriched at the furrow canal, and expression strongly increases from cycle 13 to cycle 14. Thus, spatial and temporal distribution of Slam correlates with invagination of the cellularisation furrow (Stein et al., 2002; Lecuit et al., 2002; Wenzl et al., 2010). This correlation seems to be relevant, since *slam* mutants show defects in cycle 14 but not in cycle 13. Firstly, we investigated the time of accumulation of Slam at furrows. Secondly, we wondered whether Slam accumulates differently at "old" furrows, which enclose pairs of daughter nuclei, and "new" furrows, which separate corresponding daughter nuclei. To this aim, we constructed a GFPslam fusion protein, which was expressed with a maternal tubulin promoter. GFPslam is fully functional, since it complemented the *slam* mutant phenotype in cellularisation. GFPslam recapitulated localisation of endogenous Slam during mitosis 13 and interphase 14 (Fig. 4A). Time-lapse recording of embryos expressing GFPslam revealed a dynamic distribution. GFPslam accumulated at the furrow canal as well as in particles in the basal cytoplasm. By the end of cellularisation, GFPslam levels gradually decreased similar to levels of endogenous Slam. During syncytial cycles, GFPslam marked metaphase furrows and margins of somatic buds in interphase (data not shown). In mitosis

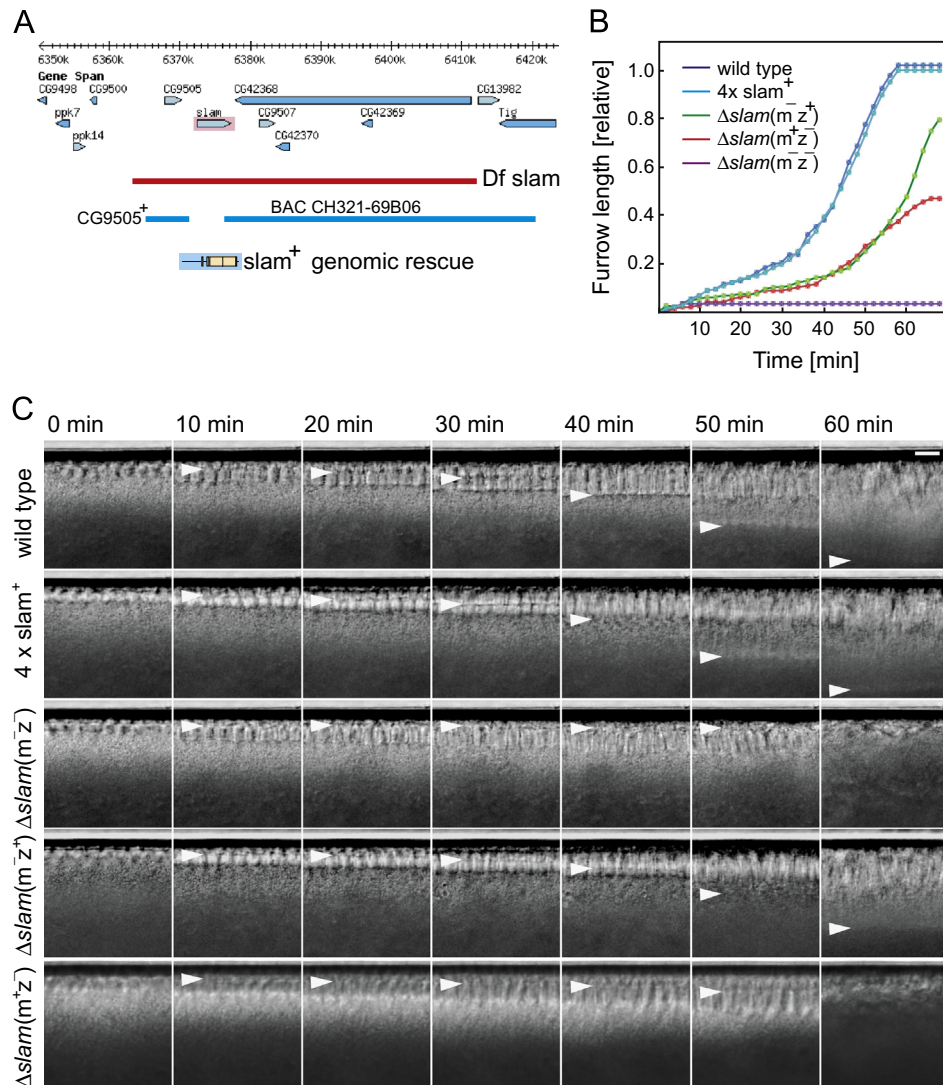


**Fig. 1.** *slam* is required for furrow formation and invagination. (A) Scheme of the *slam* genomic region according to the annotation in FLYBASE. A new deletion including *slam* and marked in red, was generated by Flippase mediated recombination of two Frt containing transposons in trans. Proximal and distal genes were rescued with transgenes of the indicated regions (CG9505, BACCH321-69B06). The *slam* rescue transgene comprises about 8 kb genomic region between the distal and proximal neighbours. (B) Time course of furrow invagination in embryos with indicated *slam* genotypes. Invagination was quantified by the distance of the furrow canal from the periphery in time lapse recordings with wide field optics. (C) Time lapse recordings of embryos with indicated *slam* genotype. The arrow head marks the position of the furrow canal. m maternal *slam*, z zygotic *slam*. 4 × *slam*<sup>+</sup>, two transgenic and two endogenous *slam* copies.

13, Slam marked the tip of the metaphase furrow (Fig. 4B). Labelling persisted during retraction in telophase and appearance of the interphase furrow (Fig. 4B, C). Due to this continuous labelling with GFPslam, corresponding daughter nuclei could be recognised by GFPslam staining at the "old" furrow. GFPslam accumulated at "new" borders between the daughter nuclei after a few minutes (Fig. 4B, red arrow, C, yellow circle). At the onset of cellularisation, GFPslam appeared in a particulate pattern. The punctae were very dynamic and variant in size and intensity. We were not able to track single particles. Later in cellularisation, GFPslam distribution became smooth and uniform.

GFPslam accumulates at the "new" furrows later than at the "old" furrows. We conceive two possibilities for this difference. The plasma membrane may fold into the plane of the nuclei between corresponding daughter nuclei later than the "old" furrow, which is derived from the metaphase furrow. Alternatively, Slam protein accumulates later at the "new" furrow than at the "old" furrow, although the plasma membrane would be present between the corresponding daughter nuclei. We used double labelling with Cherry-Slam and a GFP-tagged integral membrane

protein to distinguish these two possibilities. We used the integral membrane protein E-CadherinGFP, because E-CadherinGFP is not restricted to junctions at the onset of interphase 14 (Fig. 5A). Together with CherrySlam, E-CadherinGFP labelled the "old" furrow enclosing corresponding daughter nuclei (Fig. 5A, T=1 min). After about 3–4 min, a diffuse E-CadherinGFP signal was visible between corresponding daughter nuclei. No clear CherrySlam signal was observed between corresponding daughter nuclei at this time. This indicates that the plasma membrane, which was labelled by E-CadherinGFP, moved into the plane of the nuclei. The diffuse E-CadherinGFP signal at 3–4 min coalesced into a sharp line after 6 min. At the same time, diffuse and weak CherrySlam signal appeared between the corresponding daughter nuclei and coalesced into a sharp line slightly later. At T=6 min, corresponding daughter nuclei could not be identified by E-CadherinGFP signal, anymore. In contrast, a difference in CherrySlam signal at "old" and "new" furrows was clearly visible at 6 min (Fig. 5A). This difference in labelling indicates that Slam accumulates between corresponding daughter nuclei after the membrane folded into the nuclear plane. These data suggest that Slam does

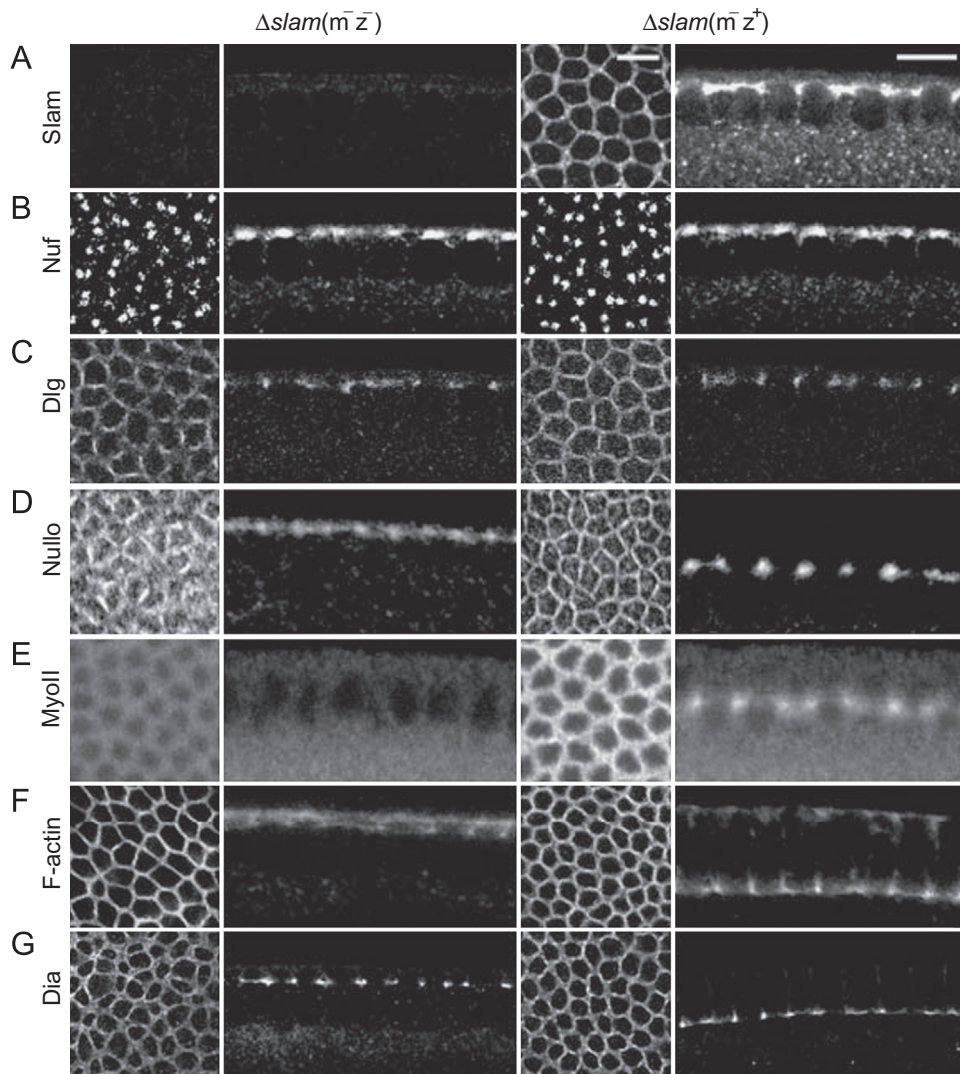


**Fig. 2.** Markers of the furrow in *slam* mutants. Embryos from females with *slam* germline clones crossed with males heterozygous for a *slam* deficiency. Embryos with zygotic expression of *slam* were identified by Slam staining. Fixed embryos were stained for (A) Slam and one or two of the indicated markers, (B) Nuf, (C) Dlg, (D) Nullo, (E) non muscle myosin II, (F) F-actin, (G) Dia. The insets show the surface view. m maternal *slam*, z zygotic *slam*. Scale bar 10  $\mu$ m.

not define and trigger initial formation of the furrow. Slam may rather be involved in later aspects of the invagination process, such as recruiting RhoGEF2 or Myo II to the furrow.

We have no indication for directional movement of Slam towards the furrow, as we were not able to track the movement of Slam punctae. We tested whether vesicular transport is directly or indirectly involved in Slam accumulation by analysing GFPslam dynamics in *shibire* (*shi*) embryos. *shi* embryos are mutant for the GTPase Dynamin (Swanson and Poodry, 1981; Pelissier et al., 2003; Fabrowski et al., 2013). *shi* is assumed to have a specific role during "slow phase" of furrow invagination by promoting membrane turnover in the furrow (Pelissier et al., 2003). As *shi* is a conditional mutant, we shifted the embryos to non-permissive temperature (32 °C) shortly before cellularisation and recorded GFPslam dynamics (Fig. 5B). Although GFPslam was maintained in a furrow array, the "new" furrow between corresponding daughter nuclei was frequently absent or did not form completely. This led to enclosure of the two corresponding daughter nuclei into one cell (Fig. 5B). These data provide further functional evidence for the notion that "old" and "new" furrows are different. Furthermore, these data indicate that *shi* and *shi*-dependent vesicular trafficking

is important for new accumulation of Slam at the "new" furrow. In contrast, *shi* seems to be less important for maintenance of Slam furrow association.

#### *nuf* is required for Slam accumulation at the furrow canal

Having shown a dependence on *shi*/Dynamin and thus on vesicular transport, we asked whether Slam localisation depended on the recycling endosome. The recycling endosome is associated with centrosomes in the blastoderm embryo (Riggs et al., 2007). Previously, it has been shown that mutation or depletion of *Rab11* or *nuf* leads to cellularisation defects (Rothwell et al., 1998; Riggs et al., 2003; Pelissier et al., 2003) and mislocalisation of RhoGEF2 (Cao et al., 2008). As RhoGEF2 localisation also depends on *slam* (Wenzl et al., 2010), we wondered whether the recycling endosome would control RhoGEF2 localisation indirectly via control of Slam localisation. We first revisited the cellularisation phenotype of embryos from *nuf* females (in the following called *nuf* embryos). Nuf protein is a homologue of Arfophilin-2 and is required for full recycling endosome function (Hickson et al., 2003). As previously reported (Rothwell et al., 1998), we observed obvious but variable

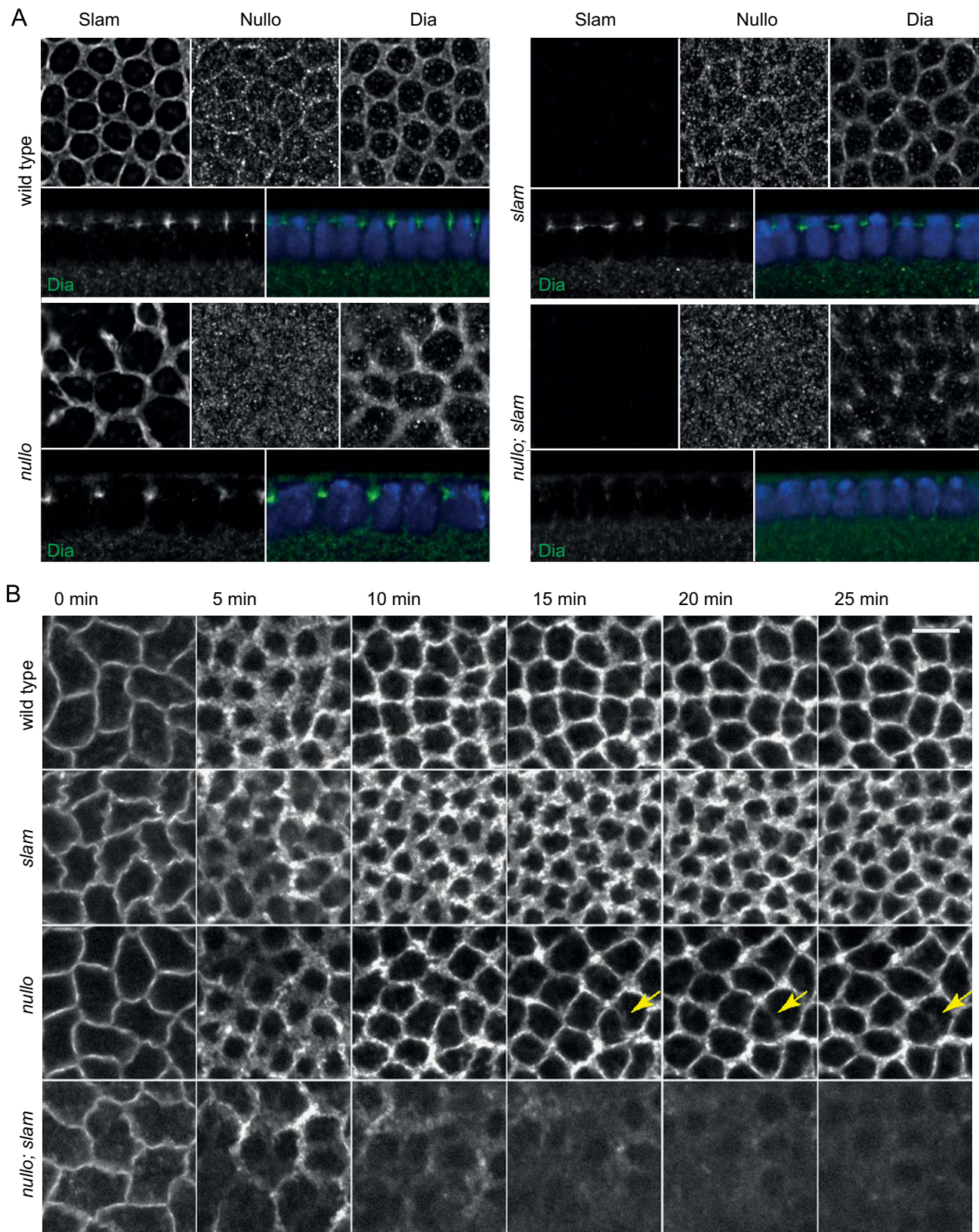


**Fig. 3.** Redundant function of *slam* and *nullo* in defining the furrow array. (A) Embryos from *nullo* heterozygous females with *slam* germline clones crossed with *slam* heterozygous males. Genotype of embryos was determined by staining for Slam and Nullo. The furrow array was visualised by Dia staining. (B) Embryos expressing E-CadherinGFP were depleted for *slam* or *nullo* or *slam+nullo* by dsRNA injection. Dynamics of the furrow array was recorded by time lapse imaging. Loss of individual furrows in *nullo* depleted embryos is indicated by arrows in yellow.

cellularisation defects. Furrow invagination was slow or aborted in about half of the embryos (Fig. 6A, B). Given Slam's membrane association (Lecuit et al., 2002), Slam may be loaded and

transported to the plasma membrane on vesicles of the recycling endosome. Such a model would predict a partial co-localisation of Slam and Rab11. Alternatively, a yet unknown Slam receptor

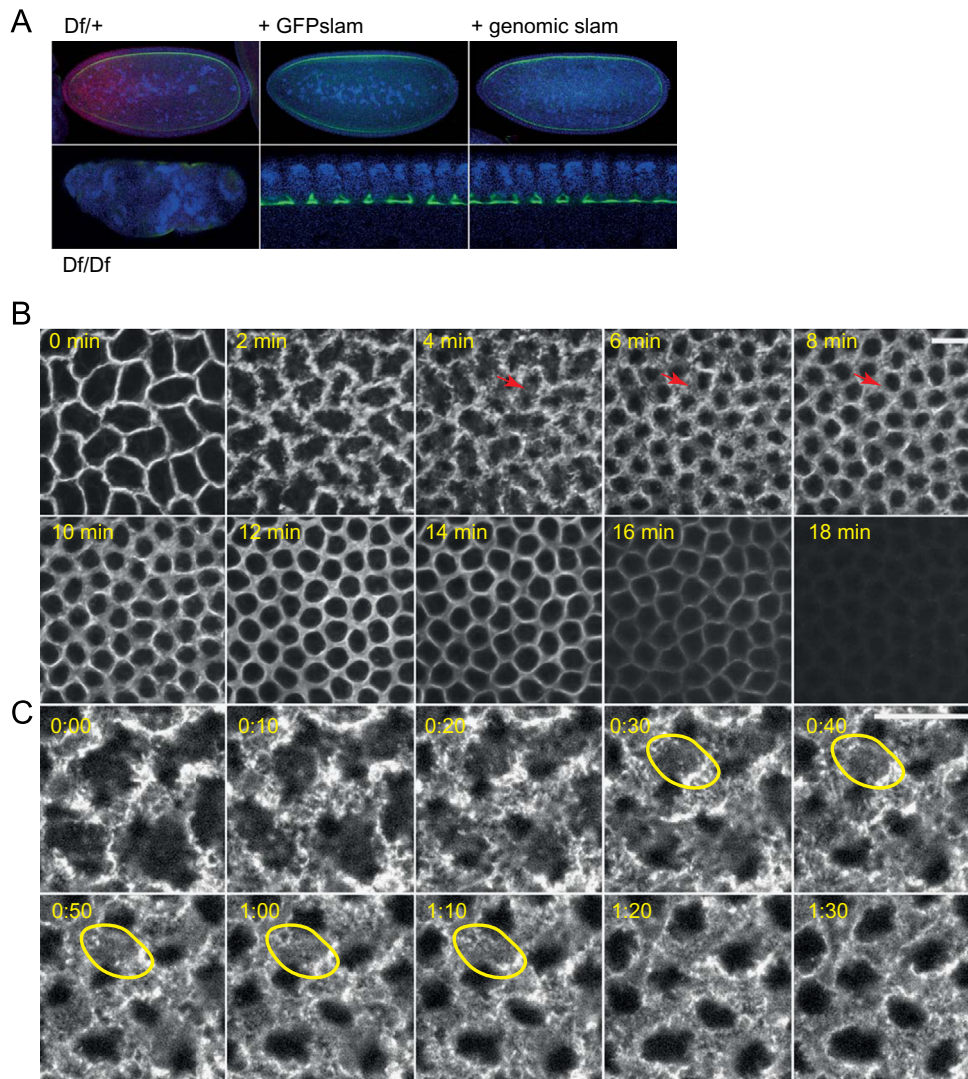


**Fig. 4.** GFPslam differentially accumulates at old and new furrows. (A) Fixed embryos zygotically homozygous for a large *slam* deficiency without or with transgenes for GFPslam driven by maternal GAL4 or the *slam* locus were stained for Slam (green),  $\beta$ -galactosidase (red) and DNA (blue). *slam* homozygous embryos were recognised by the absence of  $\beta$ -galactosidase. (B) Images from time-lapse recordings of embryos expressing GFPslam at an apical position. The arrow in red points to the position where a "new" furrow emerges. (C) Images in high magnification and temporal resolution, which show the accumulation of GFPslam at a new furrow marked by the circle in yellow. Scale bar 5  $\mu$ m.

or anchor may be transported by the recycling endosome. Slam may be enriched at the membrane only after the receptor/anchor reached the plasma membrane. Our data support the indirect model. We did not observe any overlapping staining of Rab11 and Slam in wild type and *nuf* embryos (Fig. 6C). We did not observe any (peri)centrosomal staining of Slam.

However, we observed that Rab11 staining was frequently reduced or even absent in *nuf* embryos (Fig. 6C). Importantly, we also observed unusual ectopic Slam distribution in *nuf* embryos. The ectopic Slam staining was most obvious in *nuf* embryos with a strong phenotype. Slam staining was detected at the apical cortex and along lateral furrows (Fig. 6C, D). Ectopic Slam staining was also observed in embryos with normal morphology, in which Slam punctae were detected at the lateral furrow (Fig. 6D). We also observed ectopic Slam staining in the furrow array. Sometimes, a line of Slam staining was observed between the pair of pericentrosomal RE (Fig. 6C, yellow arrow). This staining shows that Slam accumulated not only in the middle between adjacent nuclei but even above single nuclei, if the function of the recycling endosome was disturbed. This observation suggests that the information for accumulation originates

not with nuclei but with centrosomes and their associated structure.

*slam*, *RhoGEF2*, *dia* and *nullo* embryos function in separation of lateral and basal membrane domains during cellularisation (Sokac and Wieschaus, 2008b; Wenzl et al., 2010). Consistent with a role of *nuf* in controlling Slam and RhoGEF2 localisation, we found that the lateral marker Dlg spread into the furrow canal. The spreading of Dlg into the furrow canal is easily recognised by the overlapping Slam and Dlg staining (Fig. 6D, yellow arrow).

To further investigate whether Slam restriction to the furrow canal depends on the recycling endosome, we recorded GFPslam dynamics in *nuf* mutant embryos (Fig. 7A). We found clear deviations from wild type dynamics. Large particles with strong GFPslam signal were often observed next to an exclusion area prior to accumulation at the site of invagination (Fig. 7A, yellow arrow head). The exclusion area probably represents the nucleus and associated microtubules, which surround the nuclei. These large patches persisted longer in *nuf* than in wild type embryos (Fig. 7A). Whereas normally Slam accumulated in a pseudo-hexagonal array within minutes, restriction of Slam to the furrow canal was often incomplete and delayed by a few minutes in

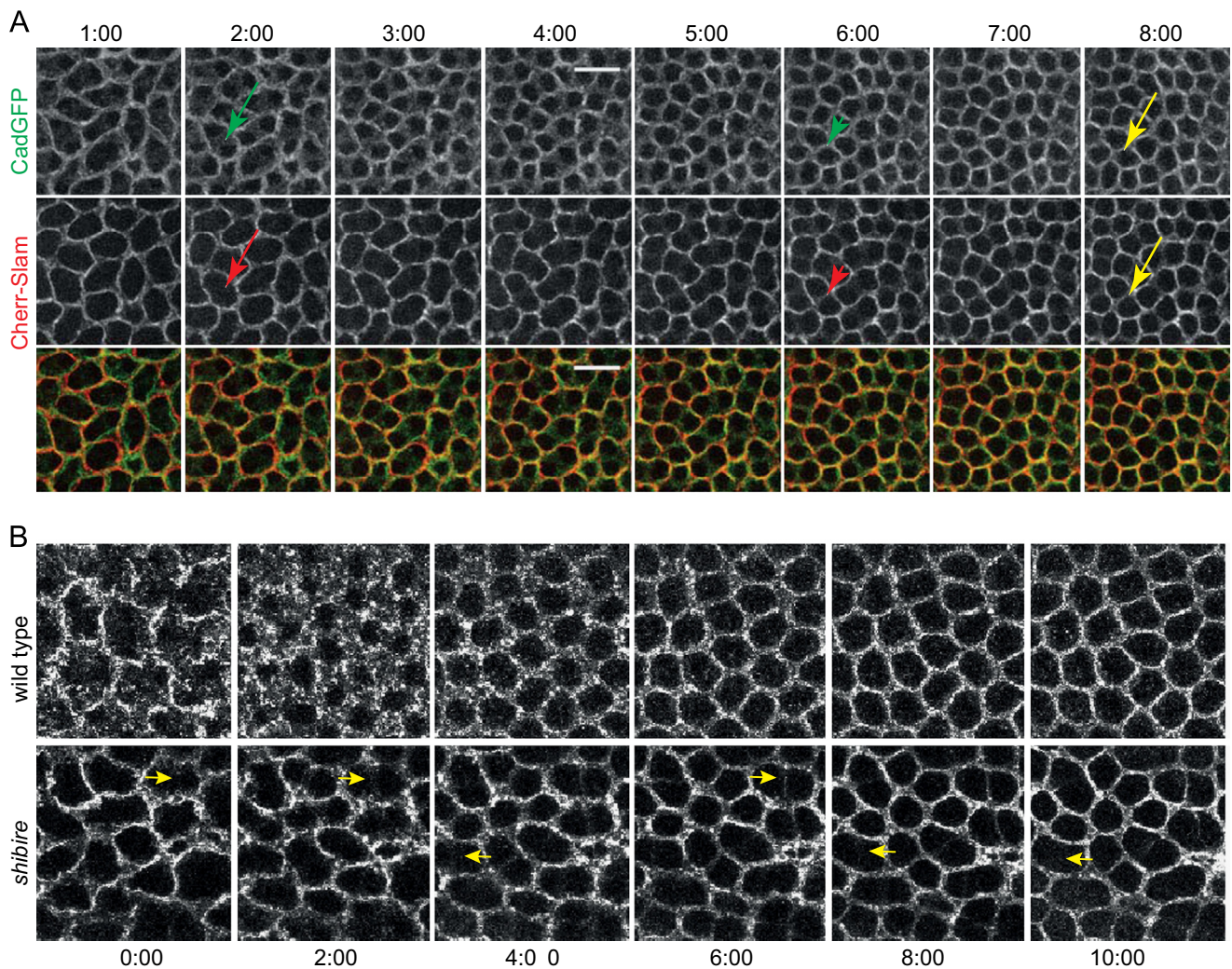


**Fig. 5.** Accumulation of GFPslam coincides with coalescence of E-CadherinGFP. Time lapse recording of embryos, which express E-CadherinGFP (white/green) and Cherry-Slam (white/red) during the onset of cellularisation. The arrows point to the prospective site of the "new" furrow, which already stains for E-CadherinGFP. The arrow head points to this site at a time when E-CadherinGFP coalesces and CherrySlam becomes visible. The yellow arrow points to a "new" furrow with strong E-CadherinGFP and CherrySlam fluorescence similar to old furrows. Scale bar 5  $\mu$ m. (B) Embryos from *shibire* and wild type female expressing GFPslam at 32 °C. Images from time-lapse recordings. Arrow in yellow points to incompletely or absent "new" furrows.

*nuf* embryos (Fig. 7A). We did not quantify this by arbitrary classifications, since the penetrance and strength of this phenotype was variable.

The control of Slam dynamics may be due to the function of Nuf on Rab11 and the recycling endosome. We interfered with Rab11 function by injection of a dominant negative Rab11 allele, Rab11S25N (serine 25 is mutated to asparagine) to test this hypothesis. It has been previously reported that injection of purified Rab11S25N protein delays furrow invagination (Pelissier et al., 2003). Using a similar approach, we found that furrow invagination was delayed in about 40% of the injected embryos (Fig. 7B, two out of five embryos) and that GFPslam restriction to the prospective region of the furrow canal was delayed by several minutes (Fig. 7C). These data suggest that the function of the recycling endosome for furrow invagination is at least partially due to timely restriction of Slam localisation to the furrow.

#### *GFPslam is mobile at the onset and stable during cellularisation*

The dynamics of GFPslam reflects steady-state levels and does not reveal the stability of membrane association. Two extreme

options for membrane association of Slam are conceivable. Firstly, Slam may accumulate at the furrow once and remain immobile and membrane bound for the remainder of cellularisation. Secondly, Slam may be mobile and constantly associate with and dissociate from the membrane.

We employed fluorescence recovery after photo-bleaching (FRAP) experiments to reveal the mobility of GFPslam in early and mid-stage cellularisation (Fig. 8). Firstly, we assayed the mobility of two markers of the furrow canal, the PDZ domain of RhoGEF2 (Wenzl et al., 2010) and Amphiphysin (Sokac and Wieschaus, 2008a; Yan et al., 2013). We photo-bleached a circular area of two to three cell diameter, which allowed us to observe the overall recovery of the fluorescence. We found that both markers rapidly and almost completely recovered within a minute (Fig. 8A–D). We adjusted the signal in the bleached region by the signal outside of the bleached region, as the Amph-YFP was weak and bleached during recording. Secondly, we tested the recovery of GFPslam during interphase and mitosis. In contrast to the PDZ domain or Amphiphysin, GFPslam fluorescence recovered slowly in interphase 13 and 14 (Fig. 8E, F, I, J). Even after 10 min, only less than half of the signal was restored. No indication for saturation was observed, as intensity

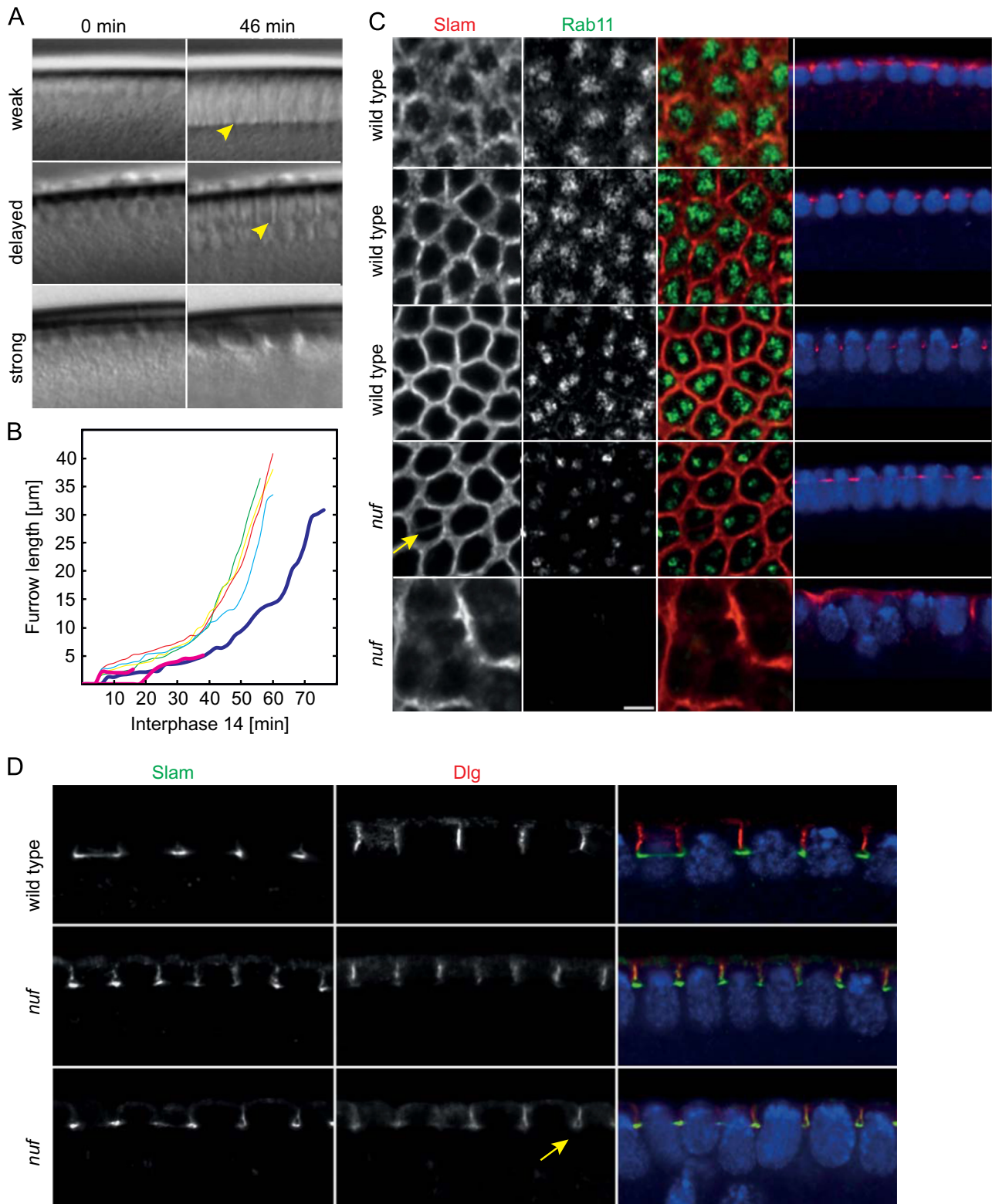


**Fig. 6.** *nuf* is required for cellularisation and restriction of Slam to the furrow canal. (A) Wide field images of embryos from *nuf* females early (0 min) and late (46 min) in cellularisation. Arrow head point to the position of the furrow canal. "weak", "delayed" and "strong" indicate phenotypic strength. (B) Furrow invagination was quantified by the distance of the furrow canal from the cortex of the embryo. Embryos with "weak" phenotypes are indicated by thin lines, "delayed" invagination by thick lines and "disrupted" invagination by pink lines. (C, D) Embryos from wild type and *nuf* females were stained for DNA (blue) and (C) Rab11 (green/white), Slam (red/white) or (D) Dlg (red/white) and Slam (green/white). *nuf* phenotypic range was uncovered by staining levels of Rab11 and distribution of Slam. (C) Arrow point to ectopic Slam staining within the centrosome pair. Scale bar 5  $\mu\text{m}$ . (D) Arrow point to a furrow canal with ectopic Dlg staining.

in the bleached region still increased after 10 min. We did not observe lateral diffusion, since the bleached area was still clearly visible after 10 min in its original size (Fig. 8I, K). We observed a

strikingly different behaviour at the transition from mitosis 13 to interphase 14. GFPslam fluorescence rapidly and completely recovered within minutes (Fig. 8G, H). This is about the stage,

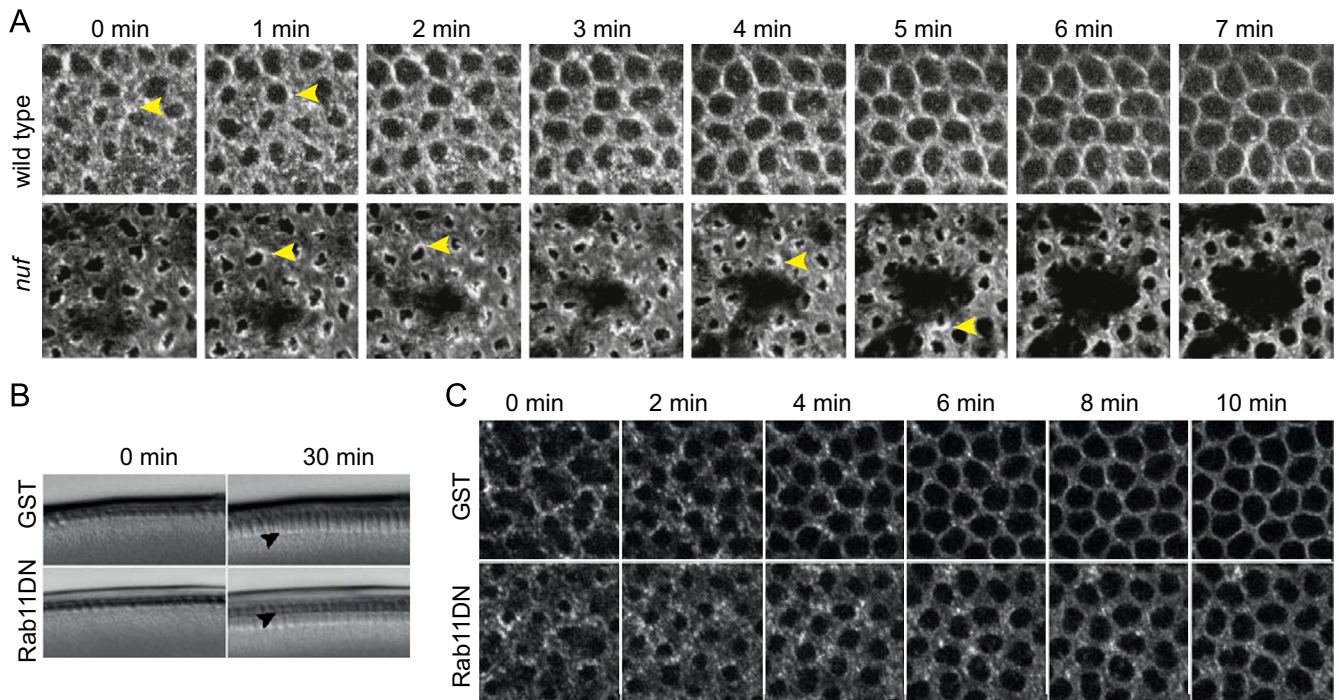


**Fig. 7.** Dynamics of GFPslam depends on the recycling endosome. (A) Images from time lapse recording of embryos from wild type or *nuf* females expressing GFPslam. The arrows in yellow point to aggregates of GFPslam. Note that such large accumulates are transient in wild type embryos but persist in embryos from *nuf* females. (B) Images from time lapse recordings of wild type embryos injected with purified GST or GST-Rab11S25N (dominant negative allele) protein. Arrows point to the cellularisation front. (C) Fluorescent images from time lapse recording of embryo expressing GFPslam and injected with GST (10 embryos) or Rab11S25N (at least 3 out of 10 embryos showed delayed Slam restriction).

when GFPslam accumulated at the position of the "new" furrow. To better define the transition from fast and complete to slow and incomplete fluorescence recovery, we performed a series of FRAP experiments with embryos with defined age. We measured the rate of fluorescence recovery by the linear slope of fluorescence recovery (Fig. 8L). The data indicate a rapid change in behaviour of Slam from high mobility at the onset of cellularisation to low mobility during the remainder of interphase.

We asked with this FRAP assay whether the recycling endosome is involved in the change of Slam mobility. Measurements were more difficult and variable than in wild type, which was due to the disordered and variable morphology of the furrow array in *nuf* embryos (Fig. 6). GFPslam signal recovered rapidly in mitosis 13 and early interphase 14 similar to wild type embryos (data not shown). In contrast to wild type, we found a high exchange rate also later in cellularisation in some of the *nuf* embryos (Fig. 9A–D). This observation suggests that *nuf* is involved in slowing down Slam fluorescence recovery during cellularisation. The faster signal recovery may be due to less restricted membrane association of Slam resulting in Slam localisation also outside of the furrow canal. For example, we observed an overall increase of GFPslam fluorescence in cellularisation outside of the bleached region. We never observed such an increase in fluorescence with the maternally expressed GFPslam in wild type embryos (Fig. 9C, D). In summary, these experiments show that *nuf* and the recycling endosome are involved in controlling the distribution and mobility of Slam, restricting the distribution to the furrow canal and limiting the exchange behaviour in interphase.

#### Centrosomes control the pattern of Slam accumulation

Finally, we asked how the initial pattern of the pseudo-hexagonal array of Slam accumulation and furrows was defined. It is very likely that the initial signal originates at the

centrosomes. Centrosomes have organiser activity in the early embryo (Raff and Glover, 1989), and the recycling endosome is arranged around the centrosomes. As described above, we observed ectopic Slam "bridges" above nuclei within a pair of centrosomes in *nuf* embryos (Fig. 6C). These observations are consistent with the hypothesis that the centrosomes provide the information for positioning of the furrow and Slam localisation at the most distant position between adjacent pairs. We analysed Slam localisation in embryos with extra (lonesome) centrosomes to test this hypothesis. Such extra centrosomes are not associated with nuclei (Peel et al., 2007). Slam accumulated between adjacent nuclei and their associated centrosomes. In addition, we detected Slam staining between the lonesome centrosomes (Fig. 10A). This Slam accumulation was functional. Staining for the lateral marker Dlg and markers of the furrow canal, F-actin and PDZ(RhoGEF2) indicated that the extra centrosomes are enclosed by a polarised furrow formed (Fig. 10A, B). The nucleus-less "cells" are organised by extra centrosomes and are not a left-over of a cell that lost its nucleus by nuclear fall-out. This was shown by time-lapse recordings of embryos expressing Sas6-GFP and GFPslam (Fig. 10C, arrow in yellow points to extra centrosome). An extra centrosome that was surrounded by a metaphase furrow in mitosis 13 was also associated with a Slam exclusion area in interphase 14 (Fig. 10C, 10 min).

Centrosomes may be required for restriction of Slam to the furrow. We aimed to functionally ablate centrosomes by application of a pulsed UV laser to a centrosome in late mitosis 13 (Fig. 10D, circle in yellow, arrow points to daughter centrosome). The centrosome lost part of its activity, at least, as no area of Slam exclusion was formed similar to the neighbouring centrosome pairs (Fig. 10D, circle in yellow). Our data show that centrosomes can organise restriction of Slam and furrow array and suggest that centrosomes are essential for Slam restriction to furrows.

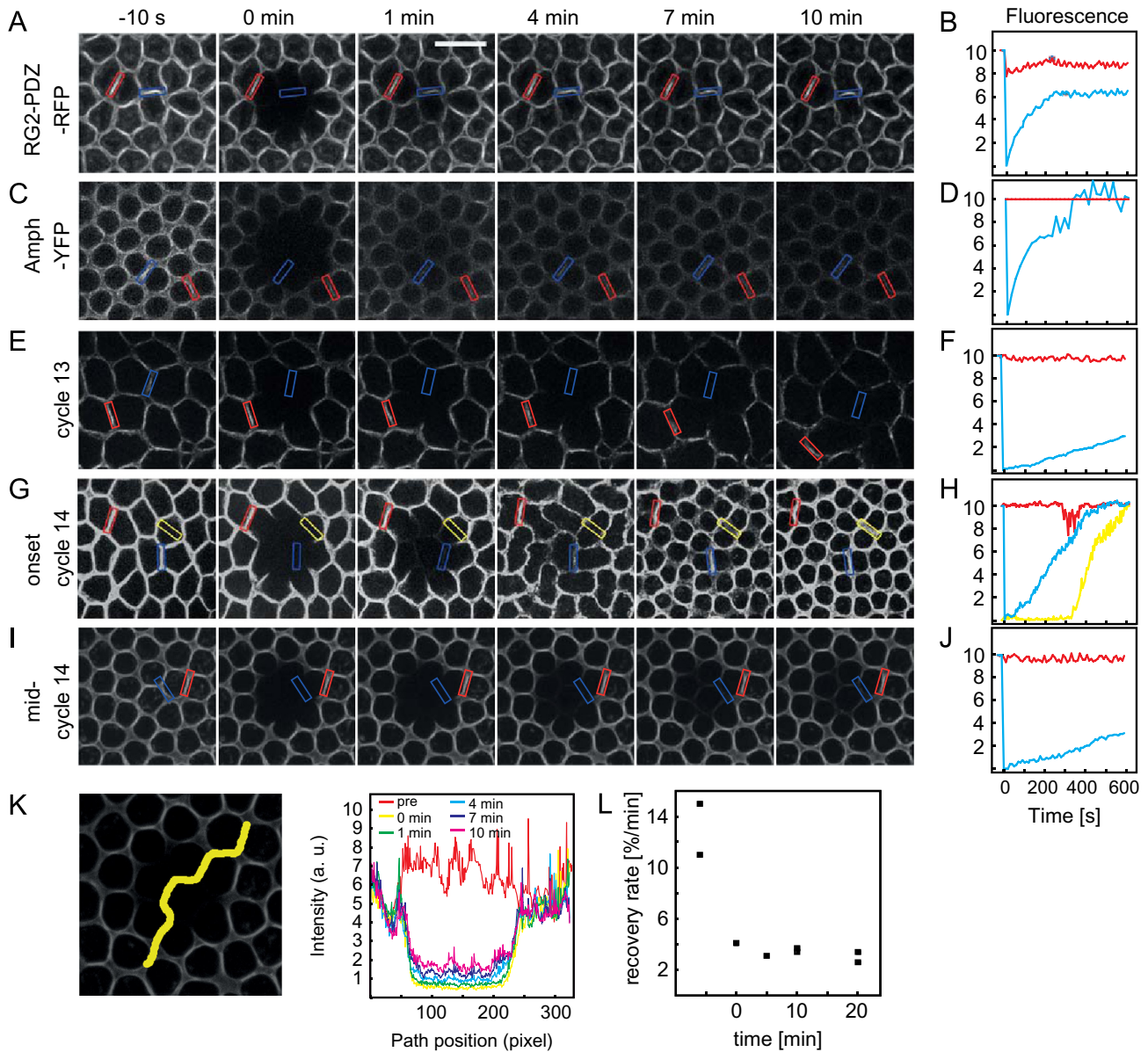


**Fig. 8.** FRAP dynamics of GFPslam. Time lapse recordings of embryos expressing (A, B) PDZ domain of RhoGEF2 fused to mRFP, (C, D) YFP-Amphiphysin in mid stage cellularisation or (E–J) GFPslam in (E) interphase 13, (G) onset of cellularisation and (I) mid stage cellularisation (interphase 14). GFPslam fluorescence was bleached in a central area and recovery was measured in relation to fluorescence in unbleached region. Fluorescence was measured in the indicated boxes (blue bleached area, red outside bleached area, yellow area of new furrows). Plots of the time courses of the fluorescence in the indicated areas (B, D, F, H, J). (D) Fluorescence inside was normalised to fluorescence outside of bleached area. (K) Fluorescence from experiment in (I) was measured along the indicated path (yellow) at indicated times. (L) Rate of fluorescence recovery in dependence of time.  $T=0$  min corresponds to furrow formation between corresponding daughter nuclei. Scale bar  $10 \mu\text{m}$ .

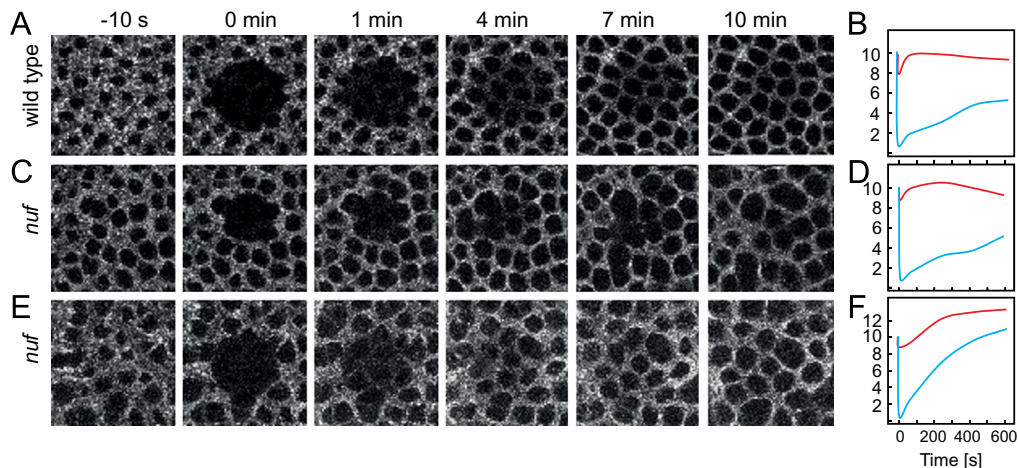


**Fig. 9.** GFPslam dynamics depends on *nuf*. Embryos from (A, B) wild type or (C–F) *nuf* females expressing GFPslam. (C) Wild type like recovery of fluorescence recovery (three of five embryos). (E) An increasing GFP fluorescence outside of the bleached area and more complete recovery (two of five embryos). Embryos (A–D) in early cellularisation. Fluorescence in area of furrow canals was measured inside (blue line) and outside (red line) the bleached region.

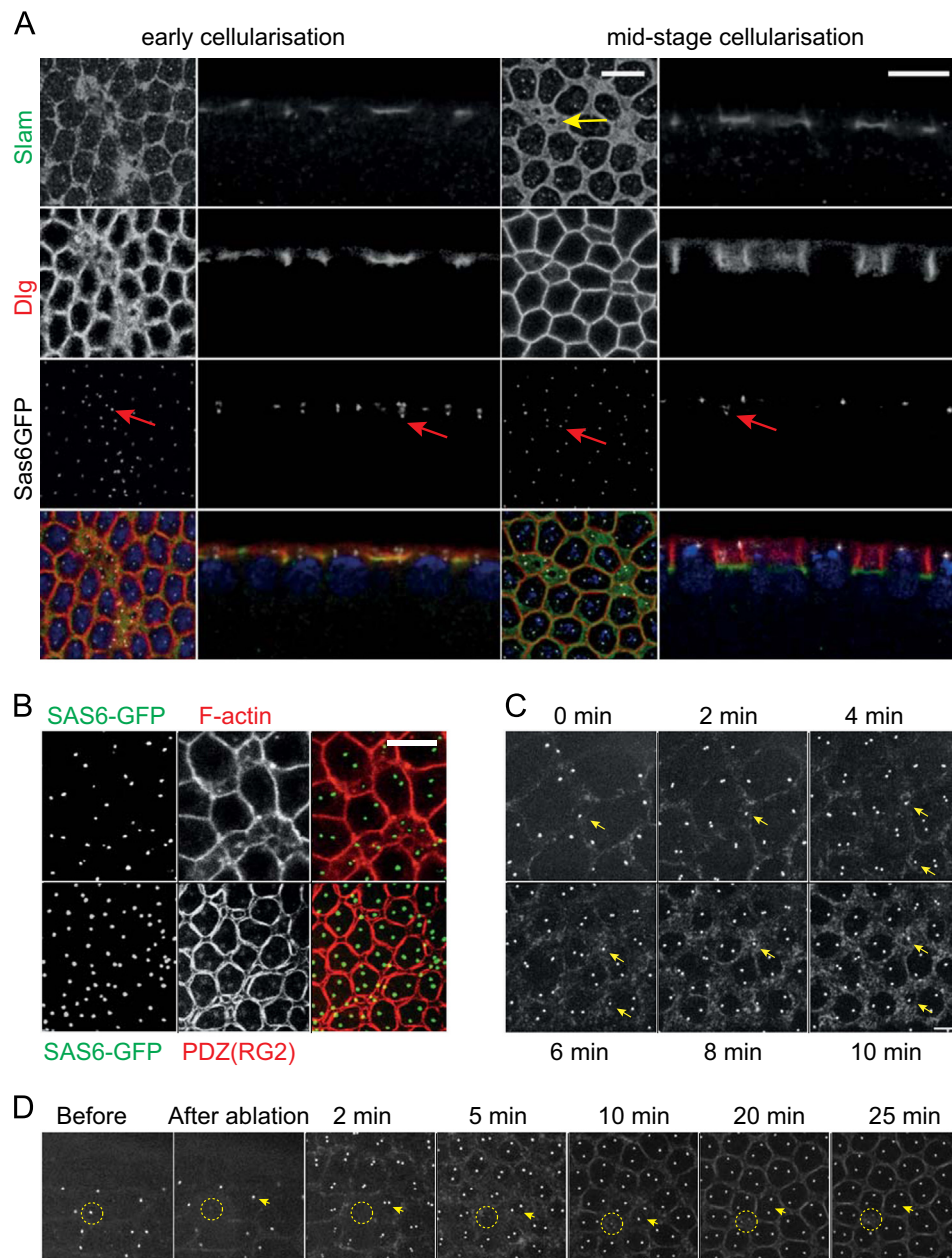


**Fig. 10.** Extra centrosomes induce additional furrows marked by Slam. (A) Fixed embryos expressing SAS6-GFP stained for Slam (white, green), Dlg (white, red), SAS6-GFP (white) and DAPI (blue) in early and mid-stage cellularisation as indicated. The arrow in red points to extra centrosomes. The arrow in yellow points to the small opening within the expanded furrow canal of cells induced by extra centrosome. (B) Fixed embryos expressing SAS6-GFP stained for SAS6-GFP (green/white) and F-actin (red/white) or PDZ(RhoGEF2)-RFP (red/white). (C, D) Images from time-lapse recordings of embryos expressing Sas6-GFP and GFPslam. (C) Arrows mark extra centrosomes. (D) Pulsed UV laser was directed to centrosome (circle in yellow) at late mitosis. The yellow arrow points to the centrosome/centrosome pair of the daughter nucleus. Scale bars 5  $\mu$ m.

## Discussion

Zygotic genes control various aspects of cellularisation and may represent trigger for the drastic changes in organisation of the cytoskeleton, membrane and cell cycle. Among the early zygotic genes, *slam* has the severest phenotype. It has been hypothesised that localisation is important for Slam function, as Slam strikingly localises to the furrow canal (Stein et al., 2002; Lecuit et al., 2002). We firstly defined the null phenotype of *slam* mutants and secondly investigated the dynamics of Slam protein and its control by the recycling endosome in order to better understand how *slam* controls membrane invagination.

A first surprising finding was the essential role of *slam* for furrow invagination but not furrow specification. Based on genetic analysis of available alleles and RNAi injection, it has been

previously proposed that *slam* promoted the speed of furrow invagination (Stein et al., 2002; Lecuit et al., 2002). By generating a *slam* deletion, we demonstrate that *slam* not only promotes but is essential for furrow invagination. Initial furrow formation and hexagonal arrangement is specified in the absence of *slam* despite the lack of a morphologically visible furrow. A possible explanation for this finding is that *slam* is not involved in defining this site, although Slam constitutes an early marker. Alternatively, *slam* may act together with another zygotic gene, namely *nullo*. We present data that are consistent with the second model. *nullo slam* double mutants lose the organisation of the furrow array as revealed by staining for Dia and E-CadherinGFP. These experiments demonstrate that *nullo* and *slam* have redundant functions. It is difficult to judge whether the disorganised Dia staining in the double mutants reflects a disorganised furrow. If this were the case, a

third zygotic input beside Slam and Nullo would be necessary. Alternatively, the disorganised Dia staining may reflect cortical localisation of Dia and tendency to aggregate. Slam and Nullo are the main signals for specification of the furrow array in this scenario. In any case, it is clear that *slam* and *nullo* collaborate for an early aspect of cellularisation in addition to their distinct functions. Such an early function of *nullo* is surprising, as *nullo* embryos show very mild defects at low temperature (Hunter et al., 2000). The strong phenotype of the double mutant is reminiscent to the loss of hexagonal pattern in embryos with depleted F-actin by injection of latrunculin (Edgar et al., 1987; Großhans et al., 2005). Our findings are also consistent with previous reports that implicated *nullo* and downstream targets of *slam* in F-actin regulation (Sokac and Wieschaus, 2008b; Wenzl et al., 2010).

A second surprising and unexpected finding was a switch in Slam dynamics from a high FRAP recovery rate in mitosis/early cellularisation to slow and incomplete recovery throughout cellularisation. Other proteins at the furrow canal such as the PDZ-domain of RhoGEF2 and Amphiphysin-YFP completely exchange within a minute during cellularisation. The recovery of GFPslam fluorescence may be due to three distinct mechanisms: (1) exchange of bleached molecules at the furrow canal with unbleached molecules from the surrounding, (2) active transport of vesicles or particles loaded with Slam, (3) localised translation. It is necessary to consider localised translation as a potential mechanism. *slam* RNA and protein co-localise at the furrow canal. This colocalisation allows for localised protein translation restricted to the site of protein localisation (Wenzl et al., 2010). As we did not detect flow of Slam punctae neither when the "new" furrow formed nor in the FRAP experiment, we do not favour the second model for fluorescence recovery. Presently, we have no data that would allow us to distinguish the models 1 and 3. Future experiments with photo-convertible tags and inhibition of translation by cycloheximide will allow us to address the potential role of localised translation.

We do not know the molecular determinants for the switch in recovery behaviour of Slam, as we have not observed indications for posttranslational modifications. However, as the exchange rate is increased in *nuf* mutants, the recycling endosome may be involved, possibly in an indirect manner. It is conceivable that restriction of Slam to the basal domain leads to a stably bound population of Slam. In contrast, unrestricted plasma membrane localisation of Slam may be based on a less stable association. It is worth noting that Slam seems to have an intrinsic affinity to membranes as Slam expressed in cultured S2 cells is cortically enriched (Wenzl et al., 2010). Slam restriction to the basal compartment may enhance and stabilise this membrane affinity.

Thirdly, it was unexpected to find differential labelling of "old" and "new" furrows by GFPslam. Such a labelling dynamics has not been described previously. For example, F-actin marks the metaphase furrow and cellularisation furrow but does not allow us to distinguish "old" and "new" furrows. Similarly, E-CadherinGFP labelling is not different in "old" and "new" furrows. The continuous GFPslam labelling of the "old" furrow and delayed and *shi* dependent accumulation at the "new" furrow suggests that there are two mechanisms for initial definition of the furrow pattern: (1) a mechanism that uses the existing information from the previous cycle, (2) a mechanism that fills the gaps in the hexagonal furrow array between the respective daughter nuclei, similar to conventional cytokinesis. The different properties of "old" and "new" furrows become obvious by their differential dependence on vesicular trafficking, as revealed in *shi* mutants. *de novo* accumulation of Slam at "new" furrows depends on vesicular budding, whereas "old" furrows are not affected under our experimental conditions. We have not investigated the situation during syncytial interphases, as *slam* has no function in these

cycles. The maternally expressed GFPslam, however, marks a pseudo-hexagonal pattern during these cycles. This syncytial staining pattern suggests that the pattern-forming process is maternally determined and that a potential Slam receptor is already present in syncytial embryos.

Our data support and further define a previously proposed model (Rothwell et al., 1999; Cao et al., 2008). It has been proposed that vesicle transport of the recycling endosome would be organised by the centrosomes. A pseudo-hexagonal pattern would emerge from the regular distribution of centrosomes. Endosomal uptake and targeted exocytosis would lead to restriction of a membranous Slam receptor to a sharply defined domain within the plasma membrane at maximal distance from the respective centrosomes. The hexagonal pattern would be completed by *de novo* formation of a "new" furrow situated between corresponding daughter nuclei. After the onset of zygotic gene expression in interphase 14, the marks would be used to accumulate new zygotic proteins such as Slam and Nullo, which would define the basal domain and trigger membrane invagination and F-actin accumulation. In addition to these functions, Slam and Nullo would maintain the furrow structure and define the basal domain. The model predicts that premature expression of the essential zygotic genes triggers membrane invagination already in syncytial interphases. We did not observe signs of membrane invagination in embryos maternally expressing GFPslam. However, precocious onset of many, if not all zygotic genes can induce cellularisation already in interphase 13 (Sung et al., 2013). It will be interesting to see which set of zygotic genes suffices to trigger furrow formation in syncytial cycles.

## Materials and methods

### Genetics

Fly stocks were obtained from the Bloomington stock center, if not otherwise noted. Following mutations and fly strains were used: Df(2L)BSC5 (*slam* deficiency), *nuf*11 (Rothwell et al., 1998), Df(1)nullo6F (Hunter et al., 2000), ubiquitin-E-CadherinGFP (Oda and Tsukita, 2001), PBac{WH}f00173, P{XP}d03327 (Exelixis collection), UASp-4xPDZ-RG2 (Wenzl et al., 2010), UASp-GFPslam (Wenzl et al., 2010), UASp-Cherry-Slam, tubulin-GAL4-VP16[67] and tubulin-GAL4-VP16[15], CyO, *hb-lacZ*, Amphiphysin-YFP (YFP exon trap, Drosophila genomics research center, Kyoto), ubiquitin-GFP-SAS6 (Peel et al., 2007). The deficiency of the *slam* locus was generated by flippase mediated recombination of two Frt sites (f00173, d03327) in trans. The successful recombinant was selected by PCR for the new hybrid transposon. *slam* germline clones were generated with a Df(2L)*slam* Frt[2L] *slam*5' rescue chromosome. The resulting cellularisation phenotype was rescued with a single copy of the *slam*-rescue transgene. The rescue of viability was tested with the following genotype: Df(2L)*slam* Frt[2L] *slam*5' rescue/Df(2L)*slam* Frt[2L] *slam*3' rescue; *slam*-rescue/+. *nullo*; *slam* double mutants were generated by crossing Df(1)nullo6F/*hs-Flp*[122]; Df(2L)*slam* Frt[2L] *slam*5' rescue/ovo[2L] Frt[2L] females with Df(2L)BSC5/CyO, *hb-lacZ* males. The *shi* phenotype was induced by shifting embryos from heterozygous females to 32 °C.

### Molecular genetics

UASp-Cherry-Slam: *slam* CDS (coding sequence) was transferred as an EcoRI-NotI fragment from pUASp-GFPslam (Wenzl et al., 2010) into pMT-Cherry. Then, CherrySlam was transferred as a XbaI-XbaI fragment to pUASp-K10 attB. The DNA was inserted into the attP-ZH-86Fb site (Bischof et al., 2007). *slam*5' rescue/CG9505<sup>+</sup> (2L 6365346..6370943): A BglIII-XhoI fragment including CG9505 was transferred from clone CH322-177104

(BacPac resources) to BglII-XhoI sites of pattB. The DNA was inserted into the attP-ZH-58A site and recombined with the deficiency of *slam*. The proximal transgene (*slam3'* rescue) for the synthetic *slam* deficiency was generated by inserting BACCH321-69B06 into the attP-ZH-51C site. *slam-rescue* (2L 6370196..6378843): The region was amplified by PCR with primer pairs PL7/8 (adding a SpeI site) and PL9/10 (adding a NotI site) from BAC-RP98-5J04 (BacPac resources) as two overlapping fragments. Following digest with SpeI, KasI and NotI, the *slam* region was cloned into the SpeI and NotI sites of pBKS and sequenced. Then, the 8.6 kb insert was transferred as a SpeI-NotI fragment into the HpaI (blunt) and NotI sites of pattB. The transgene was inserted into the attP-ZH-86Fb site. dsRNA for *slam* and *nullo* were synthesised by in vitro transcription with T7 RNA polymerase and a PCR generated template with flanking T7 sites as described previously (Lecuit et al., 2002; Großhans et al., 2005). A Rab11-S25N dominant negative clone was generated by site-directed mutagenesis by PCR with overlapping primers followed by DpnI digest. Template was Rab11 cDNA in pBK (GM06568, Genomic resource center). Wild type and S25N Rab11 clones were transferred into the BamHI site of pGEX4T1 with InFusion cloning (Clontech).

#### Rab11 protein expression

GST, GST-Rab11 and GST-Rab11S25N proteins were expressed in *E. coli* BL21DE (0.2 mM IPTG, 18 °C, overnight). Following lysis in 50 mM Tris-HCl [pH 8], 100 mM NaCl with a microfluidizer and addition of 1 mM DTT, GST proteins were purified from the soluble fraction by GSH affinity chromatography (GSTrapHP, GE Healthcare; wash buffer 50 mM Tris/HCl [pH 8], 500 mM NaCl, 1 mM DTT, elution buffer 50 mM Tris/HCl [pH 8], 50 mM NaCl, 10 mM glutathione, 1 mM DTT). After buffer exchange to PBS with PD10 columns (GE Healthcare), the protein was concentrated to 1 mg/ml and injected into GFPslam embryos.

#### Histology

Embryos were fixed by 4% formaldehyde or heat/methanol and stained according to standard procedures (Wenzl et al., 2010). Following antibodies were used: Slam (Brandt et al., 2006), Dia (Großhans et al., 2005), Dlg (4F3, Hybridoma center), Rab11 (Sathoh et al., 2005), Nuf (Riggs et al., 2007), Nullo (5C3-12, Hybridoma center), MyoII (Mechler, Heidelberg),  $\beta$ -galactosidase (Sigma). Secondary antibodies were IgG from goat coupled with Alexa dyes (Invitrogen, 4  $\mu$ l/ml). F-actin was stained by Phalloidin coupled with Alexa dyes (Invitrogen). Specimen were mounted in Aquapoly-mount.

#### Microinjection

Embryos were microinjected as previously described (Großhans et al., 2005). For RNAi injection (at about 5 mg/ml) more than 50 embryos per experiment were injected in presyncytial blastoderm stage and scored or fixed in cellular blastoderm stage. Rab and GST proteins (at 1 mg/ml) were injected into syncytial embryos and scored by wide-field and fluorescent time-lapse recording.

#### Microscopy

Time lapse recording with differential interference contrast and fluorescent optics were recorded with a Zeiss microscope with DIC optics and equipped with spinning disc or by a confocal microscope (Zeiss LSM780). FRAP experiments were performed with a Olympus IX81/PerkinElmer spinning disc microscope with an

attached FRAP laser or a confocal microscope (Zeiss LSM780). Images were processed with ImageJ/Fiji and Photoshop (Adobe).

#### FRAP

Due to the dynamics of the furrow, axial stacks were recorded. For analysis, appropriate layers were merged by maximal intensity projection. Fluorescence was measured in an area indicated by a fixed sized rectangle or in case of the experiment with *nuf* mutants in the complete area of the furrow canal and corrected by subtracting background intensity. The fluorescence measurements were not corrected or adjusted for overall loss of signal, except for the experiment with AmphYFP. Rate of fluorescence recovery were calculated by linear regression of the fluorescence recovery. Recovery refers to the fluorescence outside of the bleached area.

#### Centrosome ablation

Dechorionated embryos expressing SAS6-GFP and GFPslam were aligned on agar, transferred to a cover slide and covered with halocarbon oil. Very little glue was used on the cover slide as it reduced the efficiency of the UV laser. Centrosomes were ablated in anaphase of mitosis 13 with a 355 nm pulsed UV laser (4  $\times$  200 ms, 30%) during recording mode on an inverted spinning disc microscope (Zeiss, 63  $\times$ , NA 1.3). The UV laser (DPSL355/14, 70  $\mu$ J/pulse, Rapp Optoelectronic) was introduced from the epiport of the microscope and controlled by an independent scanning head (Rapp Optoelectronic). Following ablation, axial image stacks covering 2  $\mu$ m were recorded, processed and merged with Fiji/ImageJ.

#### Acknowledgements

We thank K Basler, A Müller, J Raff, D Ready, W Sullivan and the Developmental Studies Hybridoma bank at the University of Iowa, the Bloomington Drosophila stock center, the Drosophila genomics research center, Kyoto, the BACPAC resources at Children's Hospital Oakland and the Genomic Resource center at Indiana University for discussions, materials or fly stocks. This work was in part supported by the Deutsche Forschungsgemeinschaft (SFB 860/TP A9).

#### References

- Afshar, K., Stuart, B., Wasserman, S.A., 2000. Functional analysis of the Drosophila Diaphanous FH protein in early embryonic development. *Development* 127, 1887–1897.
- Bischof, J., Maeda, R.K., Hediger, M., Karch, F., Basler, K., 2007. An optimized transgenesis system for Drosophila using germ-line-specific phiC31 integrases. *Proc. Natl. Acad. Sci.* 104, 3312–3317.
- Brandt, A., Papagiannouli, F., Wagner, N., Wilsch-Bräuninger, M., Braun, M., Furlong, E.E., Loserth, S., Wenzl, C., Pilot, F., Vogt, N., Lecuit, T., Krohne, G., Großhans, J., 2006. Developmental control of nuclear size and shape by kugelkern and kurzern. *Curr. Biol.* 16, 543–552.
- Cao, J., Albertson, R., Riggs, B., Field, C.M., Sullivan, W., 2008. Nuf, a Rab11 effector, maintains cytokinetic furrow integrity by promoting local actin polymerization. *J. Cell Biol.* 182, 301–313.
- Crawford, J.M., Harden, N., Leung, T., Lim, L., Kiehart, D.P., 1998. Cellularization in *Drosophila melanogaster* is disrupted by the inhibition of Rho activity and the activation of Cdc42 function. *Dev. Biol.* 204, 151–164.
- Edgar, B.A., Odell, G.M., Schubiger, G., 1987. Cytoarchitecture and the patterning of fushi tarazu expression in the *Drosophila* blastoderm. *Genes Dev.* 1, 1226–1237.
- Fabrowski, P., Necakov, A.S., Mumbauer, S., Loeser, E., Reversi, A., Streichan, S., Briggs, J.A., De Renzi, S., 2013. Tubular endocytosis drives remodelling of the apical surface during epithelial morphogenesis in *Drosophila*. *Nat. Commun.* 4, 2244.
- Foe, V.E., Odell, G.M., Edgar, B.A., 1993. Mitosis and morphogenesis in the *Drosophila* embryo: point and counterpoint. The Development of *Drosophila melanogaster*, I. Cold Spring Harbor Laboratory Press, pp. 149–300.
- Grevenoged, E.E., Fox, D.T., Gates, J., Peifer, M., 2003. Balancing different types of actin polymerization at distinct sites: roles for Abelson kinase and enabled. *J. Cell Biol.* 163, 1267–1279.
- Großhans, J., Wenzl, C., Herz, H.M., Bartoszewski, S., Schnorrer, F., Vogt, N., Schwarz, H., Müller, H.A., 2005. RhoGEF2 and the formin Dia control the formation of the

- furrow canal by directed actin assembly during *Drosophila* cellularization. *Development* 132, 1009–1020.
- Hickson, G.R., Matheson, J., Riggs, B., Maier, V.H., Fielding, A.B., Prekeris, R., Sullivan, W., Barr, F.A., Gould, G.W., 2003. Arfophilins are dual arf/rab 11 binding proteins that regulate recycling endosome distribution and are related to *Drosophila* nuclear fallout. *Mol. Biol. Cell* 14, 2908–2920.
- Hunter, C., Sung, P., Schejter, E.D., Wieschaus, E., 2000. Conserved domains of the Nullo protein required for cell-surface localization and formation of adherens junctions. *Mol. Biol. Cell* 13, 146–157.
- Lecuit, T., Samanta, R., Wieschaus, E., 2002. slam encodes a developmental regulator of polarized membrane growth during cleavage of the *Drosophila* embryo. *Dev. Cell* 2, 425–436.
- Oda, H., Tsukita, S., 2001. Real-time imaging of cell-cell adherens junctions reveals that *Drosophila* mesoderm invagination begins with two phases of apical constriction of cells. *J. Cell Sci.* 114, 493–501.
- Padash-Barmchi, M., Rogers, S., Häcker, U., 2005. DRhoGEF2 regulates actin organization and contractility in the *Drosophila* blastoderm embryo. *J. Cell Biol.* 168, 575–585.
- Peel, N., Stevens, N.R., Basto, R., Raff, J.W., 2007. Overexpressing centriole- replication proteins in vivo induces centriole overduplication and de novo formation. *Curr. Biol.* 17, 834–843.
- Pelissier, A., Chauvin, J.P., Lecuit, T., 2003. Trafficking through Rab11 endosomes is required for cellularization during *Drosophila* embryogenesis. *Curr. Biol.* 13, 1848–1857.
- Raff, M., Glover, D., 1989. Centrosomes, and not nuclei, initiate pole cell formation in *Drosophila* embryos. *Cell* 57, 611–619.
- Riggs, B., Rothwell, W., Mische, S., Hickson, G.R., Matheson, J., Hays, T.S., Gould, G.W., Sullivan, W., 2003. Actin cytoskeleton remodeling during early *Drosophila* furrow formation requires recycling endosomal components Nuclear-fallout and Rab11. *J. Cell Biol.* 163, 143–154.
- Riggs, B., Fasulo, B., Royou, A., Mische, S., Cao, J., Hays, T.S., Sullivan, W., 2007. The concentration of Nuf, a Rab11 effector, at the microtubule-organizing center is cell cycle regulated, dynein-dependent, and coincides with furrow formation. *Mol. Biol. Cell* 18, 3313–3322.
- Rose, L.S., Wieschaus, E., 1992. The *Drosophila* cellularization gene nullo produces a blastoderm-specific transcript whose levels respond to the nucleocytoplasmic ratio. *Genes Dev.* 6, 1255–1268.
- Rothwell, W.F., Fogarty, P., Field, C.M., Sullivan, W., 1998. Nuclear-fallout, a *Drosophila* protein that cycles from the cytoplasm to the centrosomes, regulates cortical microfilament organization. *Development* 125, 1295–1303.
- Rothwell, W.F., Zhang, C.X., Zelano, C., Hsieh, T.S., Sullivan, W., 1999. The *Drosophila* centrosomal protein Nuf is required for recruiting Dah, a membrane associated protein, to furrows in the early embryo. *J. Cell Sci.* 112, 2885–2893.
- Sathoh, A.K., O'Tousa, J.E., Ozaki, K., Ready, D.F., 2005. Rab11 mediates post-Golgi trafficking of rhodopsin to the photosensitive apical membrane of *Drosophila* photoreceptors. *Development* 132, 1487–1497.
- Schweisguth, F., Lepesant, J.A., Vincent, A., 1990. The serendipity alpha gene encodes a membrane-associated protein required for the cellularization of the *Drosophila* embryo. *Genes Dev.* 4, 922–931.
- Sokac, A.M., Wieschaus, E., 2008a. Local actin-dependent endocytosis is zygotically controlled to initiate *Drosophila* cellularization. *Dev. Cell* 14, 775–786.
- Sokac, A.M., Wieschaus, E., 2008b. Zygotically controlled F-actin establishes cortical compartments to stabilize furrows during *Drosophila* cellularization. *J. Cell Sci.* 121, 1815–1824.
- Stein, J.A., Broihier, H.T., Moore, L.A., Lehmann, R., 2002. Slow as molasses is required for polarized membrane growth and germ cell migration in *Drosophila*. *Development* 129, 3925–3934.
- Hw, Sung, Spangenberg, S., Vogt, N., Großhans, J., 2013. Number of nuclear divisions in the *Drosophila* blastoderm controlled by onset of zygotic transcription. *Curr. Biol.* 23, 133–138.
- Swanson, M.M., Poodry, C.A., 1981. The shibre(ts) mutant of *Drosophila*: a probe for the study of embryonic development. *Dev. Biol.* 84, 465–470.
- Wenzl, C., Yan, S., Laupsien, P., Großhans, J., 2010. Localization of RhoGEF2 during *Drosophila* cellularization is developmentally controlled by slam. *Mech. Dev.* 127, 371–384.
- Yan, S., Lv, Z., Winterhoff, M., Wenzl, C., Zobel, T., Faix, J., Bogdan, S., Großhans, J., 2013. The F-BAR protein Cip4/Toca-1 antagonizes the formin Diaphanous in membrane stabilization and compartmentalization. *J. Cell Sci.* 126, 1796–1805.